

Applicability of a universal calculation model for the Integral Quality Monitor (IQM) System at matched machines

Kilian Michel, Thesi Roestel, Catherine Hamlin, Johannes Porzig, Jürgen Oellig

1. Introduction

The advent of dynamic treatment techniques in radiotherapy has required implementing quality assurance programs that include verifying each individual treatment plan. Growing patient numbers contribute to patient specific QA becoming more challenging and more time consuming. In addition, the trend toward multi-site centers and networks of centers encourages the introduction of beam matching across cancer clinics, elevating the logistical challenges of machine QA even more. The Integral Quality Monitor (IQM) System tackles these challenges with its virtualized and centralized network structure and a fully automated real-time patient QA workflow. Its core element, the IQM Detector, consists of a large-area wedge-shaped ion chamber which is flange-mounted at the collimator and measures a scalar, time-dependent dose-area-product per beam segment. During patient treatment, measurements are benchmarked in real-time against a predicted signal course which is pre-calculated by an independent, model-based, machine-specific algorithm, based on information in the DICOM-RT-Plan.

Extensive investigations concerning the dosimetric properties of the IQM Detector can be found in literature [1, 2]. Multiple studies have shown, that despite the IQM's dramatic reduction of measurement data complexity, the error detection sensitivity and specificity of the IQM System is as least as high as observed for conventional QA tools [3, 4, 5, 6]. Further, the influence of the chamber on beam characteristics has been thoroughly investigated [7].

This study focuses on the applicability of one universal IQM calculation model for 4 matched machines across 4 different cancer centers. These 4 centers are part of a centralized QA network at GenesisCare Spain that consists of 16 IQM Systems in total. The following properties were compared between the matched machines: (i) area output factors, (ii) beam profiles and (iii) IQM Signal calculation performance for clinical VMAT treatment plans.

2. Materials and Methods

All measurements were acquired at a beam energy of 6MV on Elekta VersaHD Linear accelerators equipped with Agility collimators with 160 MLC leaves. Each Linac was assigned to a specific IQM Detector.

The GenesisCare Spain physics team declared "Linac 1" to be the reference linac for machine matching. "Linac 2", "Linac 3" and "Linac 4" are the other three matched Linacs.

2.1 Area output factor (AOF) measurements

The IQM signals from 154 rectangular fields, ranging from 1x1 cm² to 30x30 cm² (see Figure 1) were measured twice for 2 of the matched machines as well as for 9 other, unmatched machines. All measurement signals were normalized based on the signals of a 10x10cm² calibration field at 50MU, to mitigate the effect of (i) different electrometer gains of the IQM Detectors and (ii) different machine outputs per Linac. As a quality criterion, the relative standard deviation of IQM Signals was assessed for each AOF-field.

The AOF measurements from the 2 matched machines were averaged to become the area output factor (AOF) determination for the universal IQM calculation model to be used with all 4 matched machines. Once the universal IQM calculation model was complete, the normalization factor (i.e. the proportionality constant linking the absolute measured IQM Signal and the raw-calculated MU-area-product) was adjusted for each of the 4 IQM Detectors, to account for slight discrepancies in electrometer gains (in a range of $\pm 1\%$).

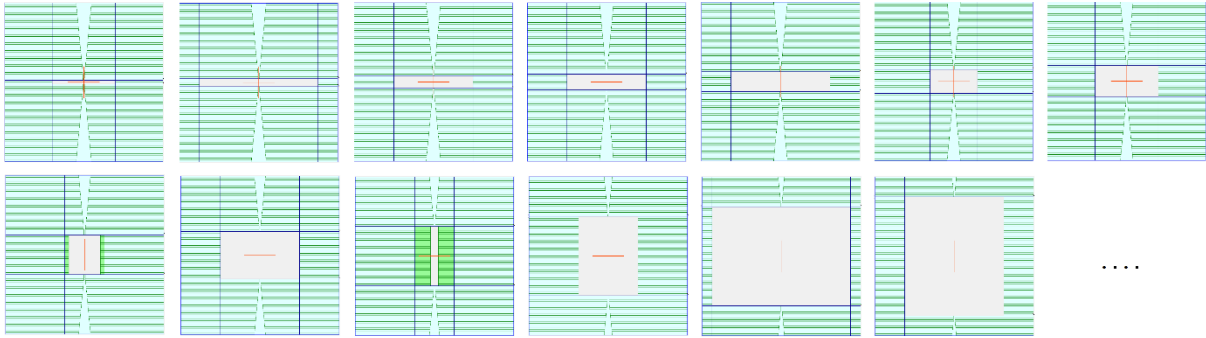


Figure 1 Example apertures which are commonly employed to empirically determine an array of Area Output Factors (AOF). The AOF is a basic requirement for the machine-specific commissioning of the IQM calculation algorithm.

2.2 Beam profile acquisition

The 40x40 cm² in-plane and cross-plane profiles were measured at 4 matched machines with a water tank (at an SSD of 100cm and D_{max}) for model comparison:

$$Symmetry_{Water-Tank} = |Relative Dose_{+150mm} - Relative Dose_{-150mm}|$$

$$Flatness_{Water-Tank} = \frac{1}{2} * (Relative Dose_{+150mm} + Relative Dose_{-150mm})$$

The average of the profiles for the reference machine (Linac 1) was included in the universal beam model for the IQM calculation algorithm, after converting the average profile from an in-water to an in-air measurement using an in-house Microsoft Excel™-based tool.

Further, the beam profiles of all 4 matched machines were measured with IQM. Each of the 4 Linacs was measured with a different IQM Detector, using the “IQM QA-Plan” that consists of a series of 4x4 cm² aperture placed strategically around the entire 40x40 cm² field area (see Figure 2). In-plane (|) symmetry and flatness values were derived from equidistant apertures along the central axis of the chamber in the non-gradient direction, expressing the signal values for these equidistant apertures relative to the “central axis aperture”:

$$Symmetry_{IQM, in-plane} = |Relative\ Signal_{+140mm(l)} - Relative\ Signal_{-140mm(l)}|$$

$$Flatness_{IQM} = \frac{1}{2} * (Relative\ Signal_{+140mm(l)} + Relative\ Signal_{-140mm(l)})$$

While the IQM QA plan data does not lend itself to deriving symmetry in the cross-plane (–) direction because of the IQM's gradient a coarse proxy is available. (Note that rotating the collimator 90° is suggested for acquiring cross-plane data, but this data was not available for these machines.) The relative signal deviations of the IQM QA Plan measurements of Linac 1 vs Linacs 2-4 were calculated. The cross-plane symmetry-by-proxy values were determined by subtracting the deviations at symmetric far off-axis locations of the central axis in the gradient-direction (cross-plane) of the chamber:

$$Symmetry_{IQM, cross-plane-by-proxy} = |Rel.\ Deviation_{+140mm} - Rel.\ Deviation_{-140mm}|$$

where the relative deviation was defined as:

$$Relative\ Deviation_{\pm 140mm} = \frac{Sig.\ Linac\ X_{\pm 140mm(-)} - Sig.\ Linac\ 1_{\pm 140mm(-)}}{Sig.\ Linac\ X_{\pm 140mm(-)}}$$

This operation was carried out under the assumption that the actual cross-plane symmetry of Linac 1 was close to 0.0%.

The deviations between IQM profiles measured for the 4 different machines were evaluated at various off-axis locations. After the universal beam model for these matched machines was implemented for the IQM calculation algorithm, the deviations between calculated and measured IQM profiles were obtained for the purpose of validating the model.

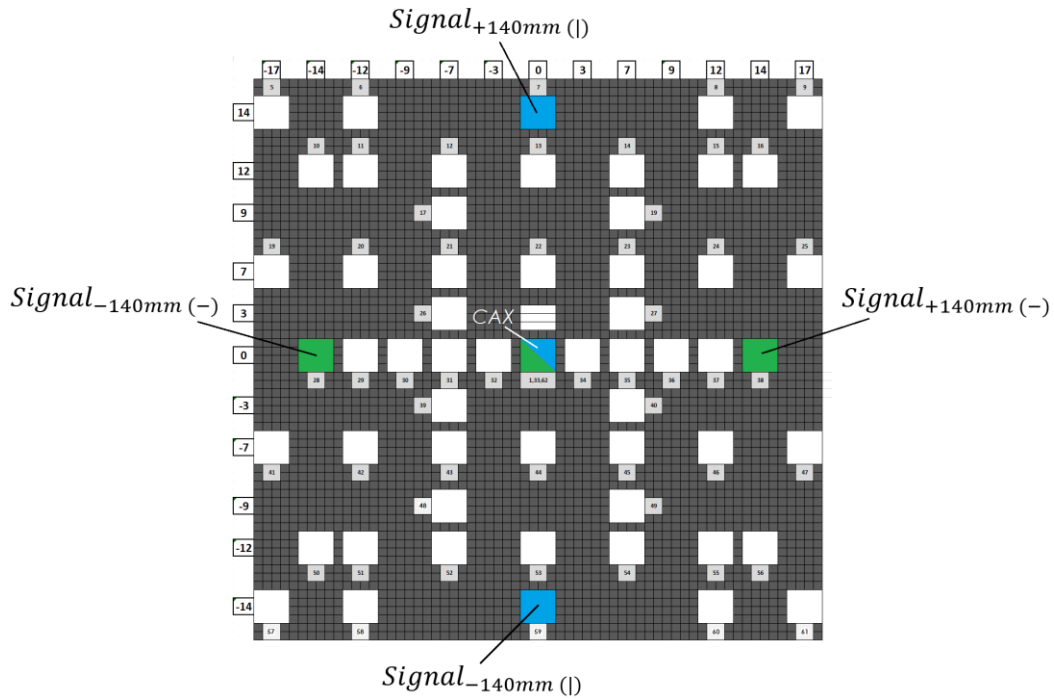


Figure 2 Geometry of the 4x4 cm² apertures of the IQM QA-plan, commonly used for IQM model validation and machine QA. The plan is intended to scan the whole 40x40 cm² beam profile covered by the active detection area of the IQM chamber. The highlighted segment's signals were used to calculate symmetry and flatness values.

2.3 Calculation performance for clinical plans

After the beam profiles of the matched machines had been evaluated, the universal IQM calculation model was employed to predict signals for 10 to 20 clinical treatment VMAT plans irradiated at each of the 4 matched machines. The plans for each Linac were chosen specifically to reflect the full range of tumor sites and plan complexity typically treated at each of the individual cancer centers.

The comparison between predicted and measured cumulative signals was evaluated based on (i) the average cumulative signal deviation, (ii) the standard deviation of cumulative signal deviations and (iii) the course of segment-specific standard deviations (SD) of cumulative signal deviations. For (i) and (ii), only the cumulative signals associated to segments 41-120 were considered. The signal variation in the initial segment range 1-40 reflects a greater variety of underlying statistical factors, including higher fluctuation and asymmetric frequency distribution due to the mathematic characteristics of the cumulative signal course, as well as systematic MU-overshooting, among other influences.

The IQM "Watch Level" defines the limit of normal machine variation and is set to reflect measurement, calculation and delivery uncertainty. It is intended to identify deviations that warrant investigation. The Watch Level corridors were determined based on the data from (iii). It consists of two parts: (1) a decreasing part at the initial phase of the irradiation (segments 1-40) and (2) a constant part for the remaining segments. A regression curve was fitted to the decreasing part of SD (1), for characterization purposes:

$$SD(\text{Segment\#}) = a * \text{Segment\#}^b$$

For (2), the standard deviation of signal deviations beyond the decreasing part of the corridor was considered. The Watch Level was empirically defined for each of the 4 matched machines by multiplying the SD with a factor, such that 98% of signal deviations lie within it (in accordance with a 2σ criteria). This allowed for a comparison of machine- and clinic-specific Watch Levels across matched machines.

3. Results and Discussion

3.1 Inter-Linac reproducibility of AOF-field measurements

The relative standard deviation of AOF-fields (SD_{AOF}) measured at two different matched machines with two different detectors reaches a maximum value of ca. 2.0%, for the smallest field size of 1x1 cm², whereas the average SD_{AOF} for all fields sizes amounts to (0.3±0.3)% (see Figure 3 (b)).

The maximum SD_{AOF} measured at the 9 un-matched machines with 9 different detectors was ca. 10.8% and the average SD_{AOF} for all field sizes was (1.7±2.0)% (see Figure 3 (c)).

To put the reproducibility between the matched machines at different sites in perspective, for commissioning the IQM calculation algorithm at a single machine, SD_{AOF} shall not exceed a value of 1.1 %, referring to measurements that are acquired back-to-back during the same session (see Figure 3 (a)). When measurements are

repeated at the same machine after several days, SD_{AOF} occasionally reach values of up to 3.0%, particularly for small fields.

The SD_{AOF} agreement between the matched machines came close to meeting the criteria for a single machine in a single session. Furthermore, standard deviations greater than 1.1% only occurred for the smallest field sizes, for which a higher signal fluctuation is to be expected due to their high relative susceptibility to inaccuracies of MLC- and Jaw-positions.

The strong reproducibility between the matched machines stands in contrast to the SD_{AOF} obtained for the array of 9 unmatched Linacs.

Given these considerations, the reproducibility of the IQM Signals of AOF-fields across matched Linacs (and their detectors) observed in this study can be considered as very satisfactory and promising for the application of a universal IQM calculation model.

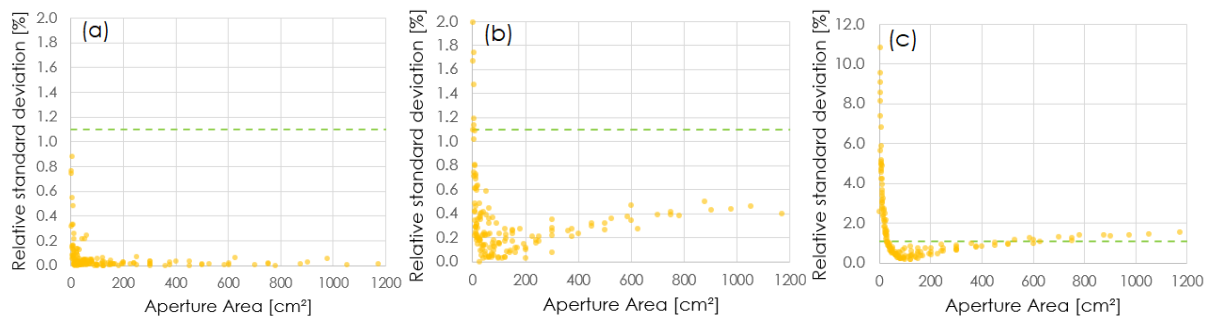


Figure 3 Standard deviations (SD_{AOF}) between IQM signals for a set of rectangular fields (AOF) relative to the referring average signal, measured at: (a) the same Linac with the same detector on the same day, (b) two matched Linacs with different chambers, (c) nine unmatched Linacs with different detectors. The single-machine single-session tolerance of 1.1% for SD_{AOF} is represented by the green, dashed line.

3.2 Conformity of beam profiles

Comparing the water-tank-measured beam profiles of the reference machine (Linac 1, universal model) vs the matched machines (Linacs 2-4) reveals measurable, yet tolerable differences (see Figure 4 (a)-(c)). The maximum flatness value of 6.6% in the water-tank data is seen in the in-plane profile of Linac 4, whereas the flatness of the reference machine's in-plane profile is 4.9%. Linac 2 and Linac 3 are in the middle, with flatness values of 6.0% and 4.9%. These values align with the relevant IQM-measured profile results, which show Linac 4 reaching the highest flatness value at 6.0%, compared to 5.1% for Linac 2 and 3 (see Table 1 and Figure 4(a)-(f)).

Linac	Water phantom In-Plane Flatness	IQM QA Field In-Plane Flatness
Linac 1 (ref.)	4.9%	5.0%
Linac 2	6.0%	5.1%
Linac 3	4.9%	5.1%
Linac 4	6.6%	6.0%

Table 1 Comparison of the in-plane beam flatness for 4 matched machines measured with a water tank vs acquired with the IQM detector. Linac 1 was declared the reference machine. The flatness values measured with IQM were derived from equidistant 4x4cm² off-axis fields along the central axis of the non-gradient direction of the chamber.

Comparing the IQM-measured profiles for Linac 2 to the IQM measured profile for the reference machine, Linac 1, we see deviations of 2.4% and -0.5% at symmetric far off-axis locations of the central axis in the gradient-direction (cross-plane) of the chamber. Relating the corresponding deviations seen for Linacs 3 and 4 (0.4%/-0.1% and 0.5/1.5%, respectively), reveals that IQM sees the largest asymmetry in Linac 2, the smallest in Linac 3, and a somewhat larger asymmetry in Linac 4, all in the same proportion relative to the water phantom symmetry values (see Table 2).

Linac	Water phantom Symmetry		IQM QA Field Symmetry	
	In-Plane	Cross-Plane	In-Plane	Cross-Plane (by-proxy)
Linac 1 (ref.)	0.0%	0.0%	0.1%	0.0%
Linac 2	0.1%	1.6%	0.7%	2.9%
Linac 3	0.5%	0.2%	1.4%	0.5%
Linac 4	0.4%	0.6%	0.1%	1.0%

Table 2 Comparison of the beam symmetry for 4 matched machines measured with a water tank vs acquired with the IQM detector. Linac 1 was declared the reference machine. The symmetry values measured with IQM were derived from equidistant 4x4cm² off-axis fields along the central axis of the (non-)gradient direction of the chamber. The IQM-measured cross-plane symmetry was approximated by comparing the QA Plan's gradient direction's measurements of the reference machine (symmetry close to 0%) to the measurements taken at Linacs 2-4.

Maximum deviations between IQM-measured profiles taken along the central axis of the gradient- and non-gradient- directions of the chamber (see Figure 4 (g)-(i)) for Linac 1 compared to those measured for Linacs 2-4 remain below 2.0% for all cases. The average deviations between all segments of the QA-plan measured for Linac1 and those measured for Linacs 2-4 are situated at (-1.0±0.8) %.

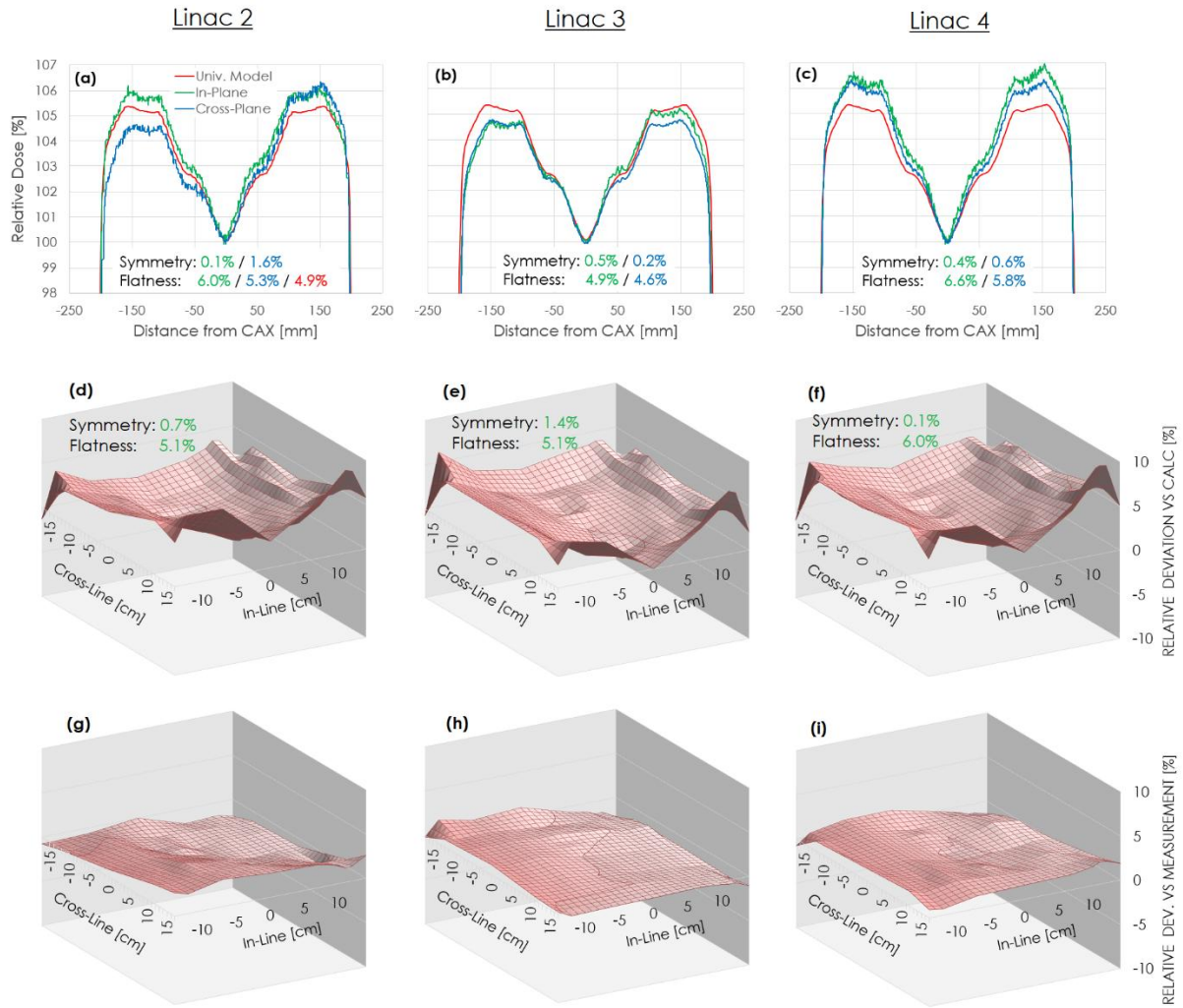


Figure 4 Comparison of beam profiles measured at 4 matched machines. Linac 1 was used as a reference machine (universal model). The in-and cross-plane profiles measured with a water tank (40x40cm², d_{max} , SSD=100cm) at Linacs 2-4 are compared against the profiles of Linac 1 (a)-(c). The IQM measurement signals of the QA-plan from Linacs 2-4 are compared against the calculation, obtained based on a universal model, commissioned for Linac 1 (d)-(f). Additionally, the QA-field measurements of Linacs 2-4 are compared against the measurements acquired at Linac 1 (g)-(i).

The reported measurement results indicate a strong correlation between beam profile properties such as symmetry and flatness measured with IQM and with a water tank. This is evidence of the clinical applicability of the IQM Detector for daily machine QA and suggests that beam profile matching can be monitored and verified reliably and consistently with the system.

3.3 Application of the universal calculation model to clinical plans

Using the universal calculation model to calculate predicted signals for all 4 matched machines, the average deviations between the final cumulative measured and calculated signals for clinical plans amounted to $(-0.2 \pm 0.6) \%$, $(0.1 \pm 0.8) \%$, $(-0.2 \pm 0.7) \%$, $(0.4 \pm 0.2) \%$, for Linac 1, 2, 3 and 4, respectively.

The histograms of deviations for all segments suggest a very similar distribution of deviations across all machines (see Figure 5 (a)-(d)).

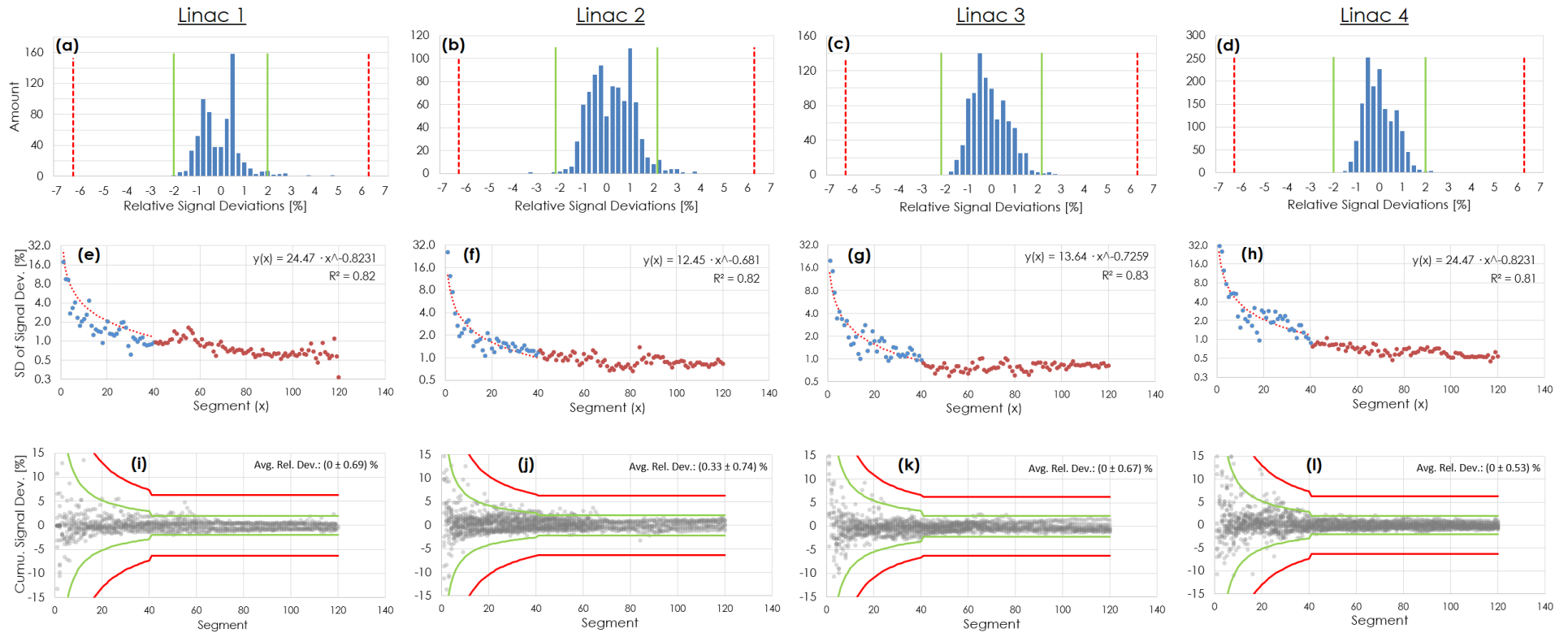


Figure 5 Comparison of deviations between measured and calculated cumulative IQM signals of machine-specific clinical plans for 4 matched Linacs. All calculated IQM Signals were predicted based on one universal calculation model. Frequency distributions of signal deviations suggest a similar dispersion and display no systematic baseline shift for all Linacs (a)-(d). The segment-dependent courses of signal deviations are illustrated with Watch and Action Levels determined independently for each machine (i)-(l), fitting a curve to the first 40 segments and applying the same empirical statistical process to the remaining segments. The resulting Watch and Action Levels show excellent agreement among the matched machines. The relevant segment-dependent courses of standard deviations suggest similar characteristics across all Linacs, concerning the fitting curves applied for the first 40 segments (e)-(h).

Due to the uniform dispersions of signal deviations, empirically determined constant Watch Levels are situated at highly comparable values: 2.0%, 2.2%, 2.2% and 2.0% for Linac 1, 2, 3 and 4, respectively.

For the decreasing part of the segment-specific standard deviation course (see Figure 5 (e)-(h)), the regression curve parameters range between $a = 12.5 \dots 24.7$ and $b = -0.68 \dots -0.82$. These differences arise from the relatively small number of data points per segment, whereas the fitting parameters are governed by high fluctuations of signal deviations.

For the sake of comparison, we reviewed historical experience for 28 unmatched machines commissioned with IQM detectors in 2018 and 2019. Their regression curve parameters ranged between $a = 8 \dots 60$ and $b = -0.5 \dots -1.3$, a far wider variation.

Both a and b are far more comparable for matched than for unmatched machines. Qualitatively speaking, the decreasing part of the corridor is comparable between matched Linacs (see Figure 5 (i)-(l)). A more extensive sample of clinical data should be assessed to quantitatively evaluate the comparability of the decreasing part of the course of standard deviations in a meaningful way.

4. Conclusion and Outlook

It was shown, that the IQM System is well usable for the evaluation of differences in beam profiles and area output factors between matched machines. Profile properties measured with a conventional water tank correlate with the corresponding metrics acquired with the IQM Detector.

Unlike for unmatched machines, it was possible to use a universal machine model with the IQM calculation algorithm to accurately predict IQM Signals of clinical plans across matched Linacs and detectors. The application of a universal calculation model reduces the amount of Linac time required for IQM commissioning measurements (i.e. area output factor determination) by a significant factor when matched machines are employed by the facility.

In addition, it was determined, that apart from the calculation model, the Watch Level settings for cumulative IQM Signals might also be universally applicable for matched machines. The comparability of the decreasing part of the Watch Level settings should be thoroughly evaluated in the future.

Bibliography

- [1] M. K. Islam, B. D. Norrlinger and J. R. Smale, „An Integral quality monitoring system for real-time verification of intensity modulated radiation therapy," *Med. Phys.*, Nr. 36 (12), pp. 5420-5428, 2009.
- [2] D. Hoffman, E. Chung and C. Hess, „Characterization and evaluation of an integrated quality monitoring system for online quality assurance of external beam radiation therapy," *J. Appl. Clin. Med. Phys.*, Nr. 18, pp. 40-48, 2017.

- [3] L. Marrazzo, C. Arilli and M. Pasler, „Real-time beam monitoring for error detection in IMRT plans and impact on dose-volume histograms," *Strahlenther. Onkol.*, Nr. 3, 2018.
- [4] M. Pasler, K. Michel and L. Marrazzo, „Error detection capability of a novel transmission detector: a validation study for online VMAT monitoring," *Phys. Med. Biol.*, Nr. 62, pp. 7440-7450, 2018.
- [5] G. Razinskas, S. Wegener and J. Greber, „Sensitivity of the IQM transmission detector to errors of VMAT plans," *Med. Phys.*, Nr. 45 (12), pp. 5622-5630, 2018.
- [6] M. Saito, N. Sano and Y. Shibata, „Comparison of MLC error sensitivity of various commercial devices for VMAT pre-treatment quality assurance," *J. Appl. Clin. Med. Phys.*, Nr. 19 (3), pp. 87-93, 2018.
- [7] B. Casar, M. Pasler and S. Wegener, „Influence of the Integral Quality Monitor transmission detector on high energy photon beams: A multi-centre study," *Z. Med. Phys.*, Nr. 27 (3), pp. 232-242, 2017.